



A highly selective anthraquinone appended oxacalixarene receptor for fluorescent ICT sensing of F⁻ ions: an experimental and computational study

MANOJ VORA^a, ANITA KONGOR^a , MANTHAN PANCHAL^a, MOHD ATHAR^b,
ASHUKUMAR VERMA^a, FALAK PANJWANI^a, P C JHA^c and VINOD JAIN^{a,*} 

^aDepartment of Chemistry, School of Sciences, Gujarat University, Ahmedabad, Gujarat 380 009, India

^bCCG@CUG, School of Chemical Sciences, Central University of Gujarat, Gandhinagar, Gujarat 382 030, India

^cCCG@CUG, Centre for Applied Chemistry, Central University of Gujarat, Gandhinagar, Gujarat 382 030, India

E-mail: drvkjain@hotmail.com

MS received 30 June 2020; revised 2 September 2020; accepted 11 October 2020

Abstract. A new anthraquinone appended oxacalix[4]arene (DAQOC) has been synthesized and characterized by different ¹H NMR, IR, ESI-MS and ¹³C NMR spectroscopic techniques. This compound was explored for its sensing abilities towards various anions. DAQOC showed selective anion sensing behaviour towards F⁻ ions which was supported by absorption as well as emission studies. Among other anions, only in the presence of F⁻ ions, a quenching in the fluorescence emission of over 79% was observed due to changes in the intermolecular charge transfer (ICT) process. DAQOC exhibited high selectivity and good sensitivity toward F⁻ ions in the presence of competing ions and the detection limit was found to be 1.23 μM. ¹H NMR titration displays that the peak corresponding to -NH protons (at 12.91 ppm) disappears upon interaction with F⁻, suggesting that the sensing mechanism follows the deprotonation route. The geometrical features of F⁻ bound oxacalixarene species were modelled by the Density Functional Theory (DFT) and NCIPLOT calculations. The findings suggested that the appended substituents including nitro groups and anthraquinone can make the calix[4]arene ring electron deficient and thereby more susceptible for F⁻ ions. Moreover, this present chemosensor has been applied for recognition of F⁻ ions from waste water samples which is of direct practical relevance.

Keywords. Chemosensor; Anions; Oxacalix[4]arene; Fluorescence; DFT calculations.

1. Introduction

Recently, there has been an upsurge in research interests on selective detection of anions due to their biological, technological, and environmental relevance.¹ Fluoride anion plays a significant role in the prevention of tooth decay.² It is also essential for the maintenance of bone health owing to its capacity to stimulate osteoblastic activity that leads to increased bone formation.³ Despite its indispensable virtues to human health, there are a number of cases reporting its acute toxicity in certain quantities, such as muscle paralysis, extremity spasms, nausea, abdominal pain,

bloody vomiting and diarrhoea.⁴ The presence of fluoride ions has also been seen in the environmental samples for organophosphorus nerve agents, for instance, hydrolysis products of sarin include fluoride.^{5,6} Therefore, new approaches for fluoride ion recognition are being developed more actively in the areas of supramolecular chemistry.⁷ In this respect, calixarene analogues are well-documented to be of significance as it possesses a developed hydrophobic cavity and facile functionalization ability at both upper and lower rims.⁸ Such modification ensures the feasibility of calixarene systems for the development of efficient and selective receptors for ions

*For correspondence

Electronic supplementary material: The online version of this article (<https://doi.org/10.1007/s12039-020-01862-6>) contains supplementary material, which is available to authorized users.

as well as neutral molecules. Oxacalixarenes are new generation synthetic host molecules of heteracalixarene family which possess outstanding complexing properties.^{9–11} The presence of oxygen atoms in oxacalixarenes, instead of methylene bridges of calixarene structures, not only changes its symmetry but also enhances its recognition character. The flexible scaffold of upper/lower rim modified oxacalixarene hosts comprising amido groups,¹² thio-ureido receptors,¹³ conjugation of amino groups with triazine rings,¹⁴ 2,3-ethylene bridged dihomooxalix[4]arene¹⁵ have been reported to detect anions. From the viewpoint of complexing ability, complexes of oxacalixarenes are spectacular from both theoretical and practical aspects, for example, Wang *et al.*,¹⁶ observed interesting ladder-like self-assembly, of tetraoxacalix[2]arene[2]triazine host molecules and demonstrated its applications of anion- π interactions. Recently, Marcos *et al.*, also reported anion complexation studies of tetraureido-dihomooxalix[4]arene where arrangements of ureido groups, resulted in chains of dihomooxalixarene molecules generated by glide planes.¹⁷ Moreover, in our previous studies, the energetics of quinolone appended oxacalix[4]arene were studied where we found that guest analyte, Cu^{2+} occupies a binding site outside the oxacalix cavity.¹⁸ Following our previous studies, we were interested in determining how the recognition mode as well as selectivity properties are influenced by appending different organic moiety to the oxacalixarene skeleton. In the present work, we have synthesized and tested another receptor, 2,14-di(N-(9,10-dioxo-9,10-dihydroanthracen-1-yl)-acetamide) tetranitro-oxacalix[4]arene (**DAQOC**) for its anionic recognition ability. The introduction of aminoanthraquinone units on the oxacalixarene structure produced a selective probe for fluoride ion detection through hydrogen-bonding interactions. Herein, the anthraquinone modified with amino groups changes the electronic energy levels of the oxacalix ionophoric fragment which opened new prospects in the design of **DAQOC** with excellent selectivity towards fluoride anions even in the presence of other competing ions. Following the first report on the use of aminoanthraquinone appended oxacalixarene as a fluorescent sensor for the selective and sensitive detection of fluoride ions, we have also substantiated their complexation abilities by computational modelling. The work has also been successfully applied for real water sample analysis to examine its possibilities for analytical applications.

2. Experimental

2.1 Materials and instruments

1-amino anthraquinone, triethyl amine, tetrabutyl ammonium salts of anions and other chemicals were supplied by Sigma-Aldrich. Silica gel and fluorescence active TLC plates (F-2009) were purchased from Merck. All the solvents employed for synthesis were commercially available and used as received without further purification. The melting points (uncorrected) were obtained from an OPTIMELT (Model: MPA100) melting point apparatus. Samples for infrared spectra were prepared as KBr pellets, spectra were recorded on Tensor Bruker 27 (Ettlingen, Germany) and expressed in cm^{-1} . $^1\text{H-NMR}$ spectra were recorded on a FT-NMR model Bruker, Avance II (500MHz) at 298 K with TMS as the internal reference. ESI-MS were recorded on micromassQuarter2 mass spectrometer. Ultra-violet absorption spectra were obtained on a Jasco V-570 UV-Vis spectrophotometer. Fluorescence spectra were recorded on HORIBA FluoroMax-4 (Xenon lamp head Xe900) spectrometer.

2.2 Synthesis and characterization of **DAQOC**

The parent 2,14-dihydroxy tetranitrooxacalix[4]arene was initially prepared by the standard protocol proposed in the literature.¹⁹ Triethyl amine (TEA, 2.2 equiv) was added to the solution of 2,14-dihydroxy tetranitrooxacalix[4]arene (0.5 g, 1 equiv) in DMSO as solvent, to which chloro acetyl derivative of 1-aminoanthraquinone (2.1 equiv) was added with vigorous stirring and the reaction mixture was stirred for 8 h at 80 °C. The reaction was monitored by TLC and after completion of reaction, the mixture was added drop wise to 1 M HCl (40 mL). The precipitate was filtered, washed with water and dried in vacuo to get the desired crude compound. The crude was purified with column chromatography using silica gel with EtOAc:Hexane (3:7) as an eluent. The fractions were separated, dried in vacuo to give **DAQOC**²⁰ (yield of 48%, Scheme 1). Melting point: 273 °C; $^1\text{H NMR}$ (500 MHz, d_6 -DMSO (δ ppm) (Figure S1, Supplementary Information) 4.11 (s, 4H), 7.22 (t, $J = 1.4$ Hz, 4H), 7.46 (d, $J = 1.4$ Hz, 2H), 7.56 (td, $J = 7.5$, 1.5 Hz, 2H), 7.94 (m, 4H), 7.98 (m, 4H), 8.27–8.18 (td, $J = 7.5$, 1.5 Hz, 6H), 9.17 (s, 2H), 12.91 (s, 2H); $^{13}\text{C NMR}$ (125 MHz, d_6 -DMSO) (Figure S2, Supplementary Information) (δ ppm: 43.5, 117.7, 118.2, 122.4, 125.1, 126.4, 127.0, 131.5, 132.1, 133.4, 134.7, 135.7, 140.2, 146.3, 156.8, 165.8, 172.8, 181.9, 186.3); Mass spectrometry m/z % (ESI-MS) (Figure S3, Supplementary Information): 1107.4 $[\text{M}+\text{H}]^+$ (calc. 1106); FT-IR (Figure S4, Supplementary Information): 3200, 3102, 2924, 1680, 1589, 1524, 1410, 1274, 1003, 833 cm^{-1} ; Elemental Analysis calculated for $\text{C}_{56}\text{H}_{30}\text{N}_6\text{O}_{20}$: C,60.77; H,2.73; N,7.59%; O, 28.91%, Found: C,60.72; H,2.86; N,7.65; O,28.97%

2.3 Spectrophotometric and spectrofluorimetric titration studies of DAQOC

The selectivity of DAQOC (stock solution of 4×10^{-5} M prepared in acetonitrile) was tested against a series of anions (2×10^{-4} M) such as F^- , Cl^- , Br^- , I^- , AcO^- , PO_4^{3-} , OH^- and $H_2PO_4^-$. The anions in the spectral studies were added as tetrabutylammonium salts in order to avoid any possible complexation of ionic species with DAQOC. The solution of anions were also prepared in acetonitrile. Equal volumes (2.5 mL) of DAQOC and each anion were prepared and added in the 5 mL volumetric flask, so that the effective concentration of DAQOC ligand is 2×10^{-5} M. Absorption and emission spectra of prepared solutions of DAQOC and that of anions were compared.

2.4 Theory and computational details

All calculations were carried out at GAUSSIAN 09 (G09) (Revision B.01) software package by using the Grimme's B97D exchange correlation functional.^{21,22} Moreover, double zeta basis set (6-31+G*) was considered for all the elements to locate the singlet ground state of the calix host structure. The optimized host structure of DAQOC (in 1,3-alternate conformation) was used for the generation of guess anionic complex (with fluoride ion) by positioning the anion in the vicinity acetamide -NH and the centroid of the anthracene and oxacalix moieties.²³ Obtained energetically stable optimized complex structure was further subjected for vibration frequency calculations to ensure that the retrieved geometries represent local minima associated with positive *eigen* values only. Further, the interaction energy

($\Delta E_{\text{binding}}$) was calculated from the single point calculations with correction for the basis set superposition error (BSSE) by using the Boys–Bernardi counterpoise method^{24,25} at the B97D/6-31+G* level. It was also of interest to examine the thermochemistry of the anion binding with the calixarene receptor; and hence we have calculated the complexation enthalpy and free energy at 298 K. Further, comprehending the role of the non-covalent interactions, it was analyzed by using NCI (Non Covalent Interaction) plot which uses the electron density and its derivatives to enable the identification and visualization of non-covalent interactions efficiently.²⁶

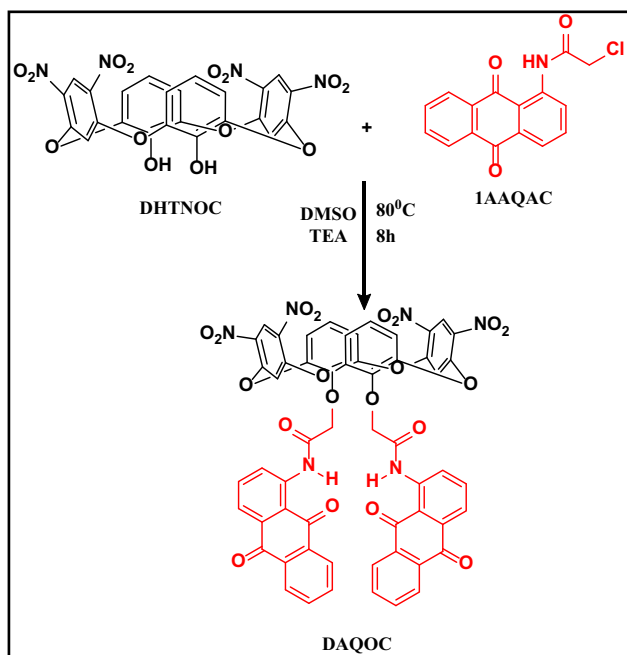
3. Results and Discussion

3.1 Synthesis of DAQOC

For the synthesis of DAQOC, 2,14-di(N-(9,10-dioxo-9,10-dihydroanthracen-1-yl)acetamide) tetranitro-oxacalix[4]arene, 2,14-dihydroxy tetranitrooxacalix[4]arene (DHTNOC) was chosen as starting material (Scheme 1). The other starting material, chloro acetyl derivative of 1-aminoanthraquinone (1AAQAC) was prepared by the reaction of 1-aminoanthraquinone with chloro acetyl chloride using chloroform as solvent and triethyl amine as base (further details in Supplementary Information). The 1H NMR of DAQOC (DMSO- d_6 solvent at 25 °C) showed the signal of -NH proton at 12.91 ppm, which indicates its hydrogen-bonding ability.²⁷ The two arms of DAQOC are covalently linked with aminoanthraquinone units with good yields. In addition to the extended pi-conjugation in the DAQOC structure, the incorporation of aminoanthraquinone moiety renders intramolecular H-bonding between the amine proton and the quinone oxygen.²⁸ According to previous reports, in comparison to other anions, fluoride ions seems to interact more strongly with a hydrogen bond donor of a receptor such as amine, hydroxyl or with amido functionalities.²⁹

3.2 Absorption and emission studies

The absorption profile of a ligand is dictated by the nature and position of its chemical substituents. Electron donating group such as amine on the anthraquinone unit induces absorption band to a longer wavelength region >350 nm.³⁰ In the present study, for DAQOC, the absorption spectrum revealed a spectral feature centred at 393 nm. On the addition of fluoride, the absorption band of DAQOC bathochromically shifts to 408 nm (Figure 1). It is



Scheme 1. Synthetic route for the synthesis of DAQOC.

well-known that large bathochromic shift is induced in anthraquinone derivatives which is caused by intramolecular charge transfer involving lone pair of electrons of the amino groups. The extent of the shift depends on the electron-donating ability of the substituents on the amino group.³¹ However, it cannot be deduced that not all the anthraquinone functional moieties exhibit this behaviour. 1-aminoanthraquinone derivatives are prone to exhibit the absence of a large wavelength shift or drastic colour change due to weaker substituent effect. In the present case, the presence of electron withdrawing -nitro substituent groups and electron rich aminoanthraquinone units broadens the conjugation in the pre-organised structure, and also modulates the photo-physical properties of the DAQOC as a host compound. Intermolecular charge transfer occurs between the oxalix ionophoric unit and the carbonyl group or the intramolecular hydrogen bonded carbonyl chelated ring of aminoanthraquinone. According to the intermolecular charge transfer (ICT) mechanism³² upon excitation of light, the absorption spectrum of DAQOC may cause red-shift in the UV-vis spectra and can be used as selective probe for F⁻ ions. The fluoride ion recognition is due to the induced deprotonation of DAQOC through hydrogen bonding interaction of -NH groups. Furthermore, the intermolecular H-bonding to investigate NH-F interactions has been substantiated by NMR titration experiments and computational results which has been discussed in the later section. The comparative interference absorption studies were conducted using other anions with DAQOC-F⁻ complex (Figure S5, Supplementary Information). The addition of other anions showed only nominal changes in its absorption maxima indicates the remarkable selectivity and that the DAQOC-fluoride ion interactions were not significant with these anions. Notably, the modification of structurally simple anthraquinone sensing moiety with the oxalix[4]arene units possessing electron-withdrawing (-NO₂ groups) changes the sensing abilities and thus accounts for selective anion recognition ability.^{29,33}

Regarding the fluorimetric response, the emission wavelength of DAQOC was observed at 508 nm under excitation wavelength at 393 nm (Figure 2). Upon the addition of F⁻ ion, the fluorescence intensity of DAQOC decreased considerably, revealing 79% quenching behaviour (Figure S6, Supplementary Information). The quenching (Figure 3) of DAQOC decreased in the presence of 1–100 fold excess of F⁻ ions, which may be due to fluorides' high charge density.³⁴ Additionally, the good sensitivity and selectivity in the fluorescence results of DAQOC is

also attributed to the presence of electron withdrawing element (O or N) bound to a carbon with α -hydrogens.³⁵ In the presence of other competitive anions, the fluorescence quenching results remained unaffected (Figure 4). Similar studies and competitive interferences studies were performed with other anions (Figure S7, Supplementary Information) and cations (Figure S8, Supplementary Information) i.e., perchlorate salts (Zn²⁺, Co²⁺, Fe³⁺, Ca²⁺, Al³⁺, Na⁺, Mg²⁺, Mn²⁺, Cr³⁺, Pb²⁺ and Ni²⁺) where, as expected none of the anions or cations exhibited any change in the emission pattern.

As only fluoride showed considerable change in emission intensity, therefore its fluorescence data was evaluated to assess its binding constant with DAQOC (Figure 5a) using the literature procedure.³⁶

$$\text{Log} \frac{F_0 - F}{F} = K_b + n \text{Log}[Q]$$

Here, K_b is the binding constant, n represents number of binding sites, F_0 and F are the relative fluorescence intensities of the complex without addition of F⁻ and with maximum concentration of F⁻, respectively. Thus, by plotting $\log (F_0 - F)/F$ versus $\log [Q]$, binding constant K_b is found. The plot of $\log [(F_0 - F)/F]$ versus $\log [Q]$ for selected fluoride has been depicted in Figure 5(b) and the binding constant of complex found to be $4.45 \times 10^{10} \text{ M}^{-1}$.

The emission spectra of 1-amino anthraquinone was inspected to determine the quantum yield of DAQOC. The reported quantum yield of 1-aminoanthraquinone was approximately 1.0³⁷ and that of DAQOC-F⁻ ions complex was found to be 0.87. It was observed that the number of emitted photons decreases with the addition of increasing concentration of F⁻ ions, that is, quenching takes place. The binding stoichiometric of DAQOC with fluoride ions was determined by the modified Job's method of continuous variation. (Figure S9, Supplementary Information). In our case, the absorbance of DAQOC and F⁻ complex approaches maximum when a mole fraction of fluoride ions was 0.5, thereby confirming 1:1 complex formation between DAQOC and F⁻ ions.

3.3 NMR titration studies

The formation of the DAQOC-F⁻ complex affects the electron transition process of aminoanthraquinone moieties and causes changes in the absorption and emission spectrum of DAQOC. Moreover, in order to gain more insights into the sensing mechanism, proton NMR titration studies was carried out. As shown in

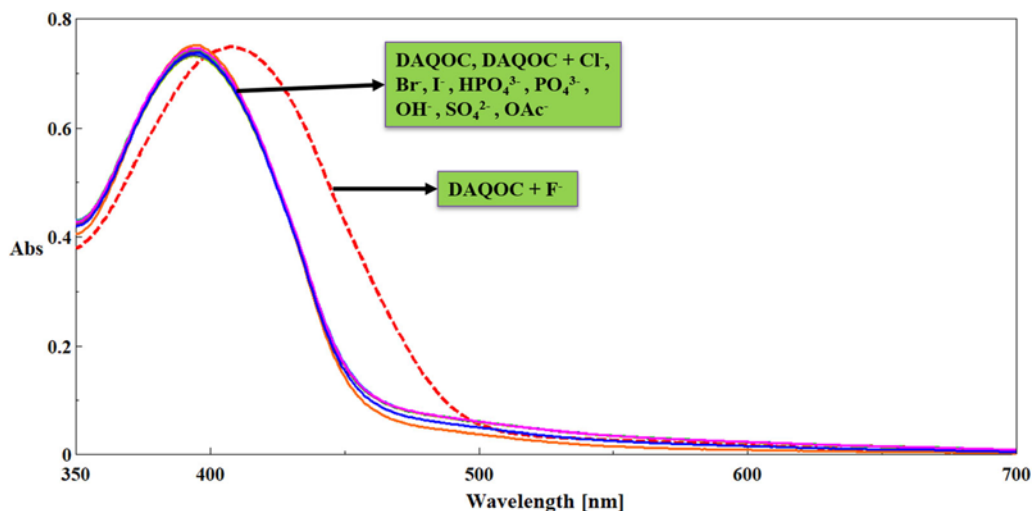


Figure 1. UV-Visible spectra of DAQOC ligand (4×10^{-5} M) with different anions (2×10^{-4} M) in acetonitrile.

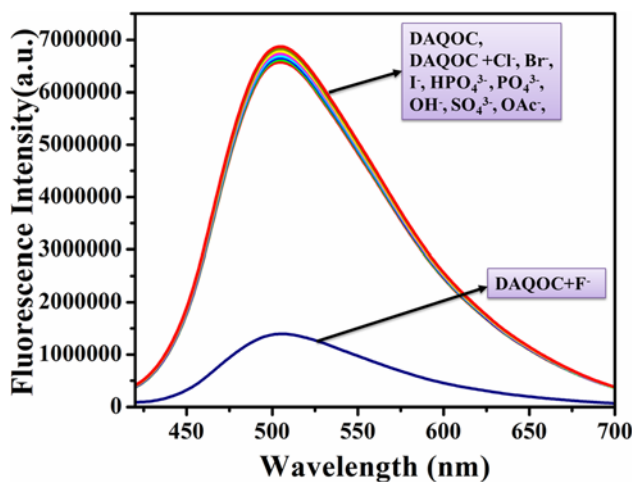


Figure 2. Emission spectra of DAQOC (4×10^{-5} M) upon the addition of F^- in acetonitrile.

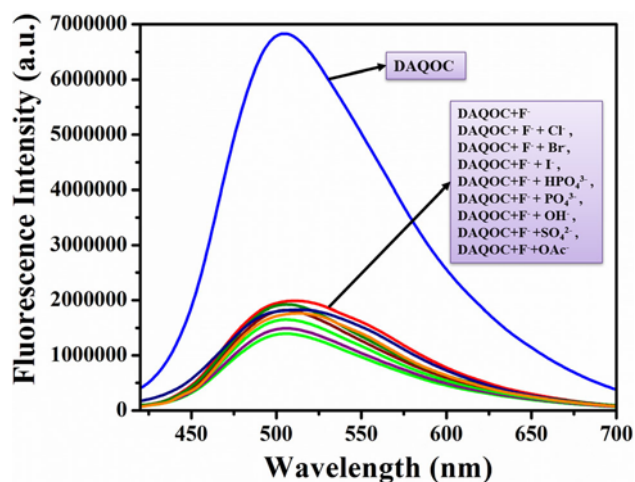


Figure 4. Emission spectral change of DAQOC- F^- (4×10^{-5} M) upon the addition of other anions.

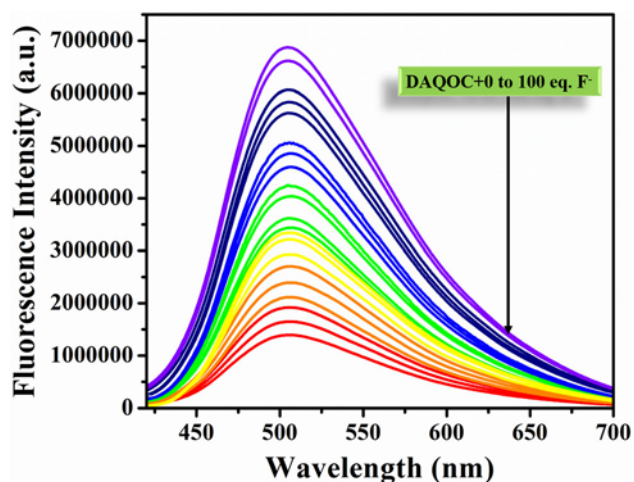


Figure 3. Emission spectral change of DAQOC (4×10^{-5} M) upon the addition of 0-100 equivalents of F^- in acetonitrile.

Figure 6, due to hydrogen bonding of F^- ions with $-NH$ group of amide linkage of DAQOC ligand, the $-NH$ peak at δ value at 12.91 ppm diminishes appreciably by gradual addition of F^- into DAQOC ligand.³⁸ In the present case, probably due to partial deprotonation, the amount of F^- (1.0 equiv.) made the signal of $-NH$ proton at 12.91 ppm disappear to a greater extent. A weak hydrogen bond interaction exists between highly electronegative F^- with $-NH$ protons which favours deprotonation and causes change in the absorption and emission spectral results of F^- ions. However, it is anticipated that further increase of the amount of fluoride ions (about ten-fold excess) should have obliterated the $-NH$ proton signal, as reported elsewhere.^{39,40}

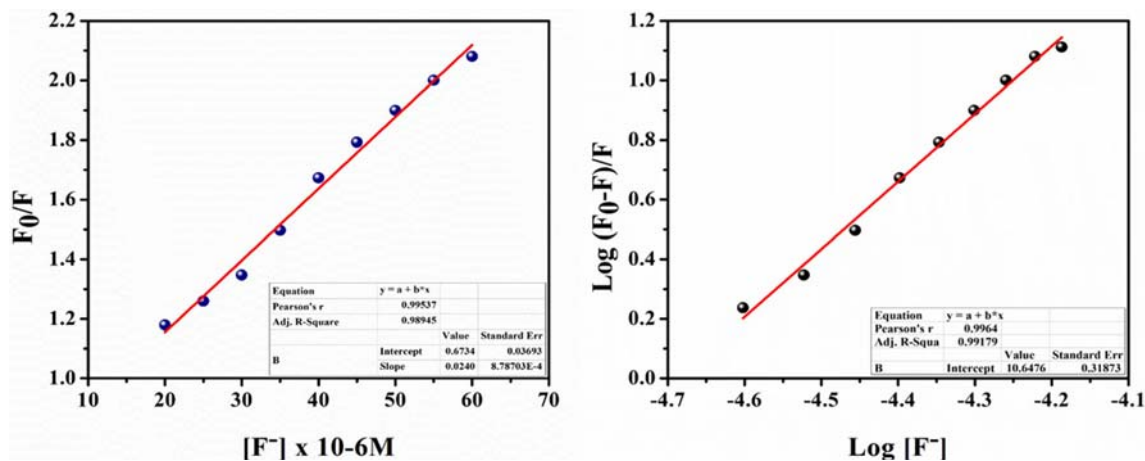


Figure 5. (a) Stern–Volmer plot (b) Modified of Stern–Volmer plot of DAQOC- F^- system (Inset: Linearity plot).

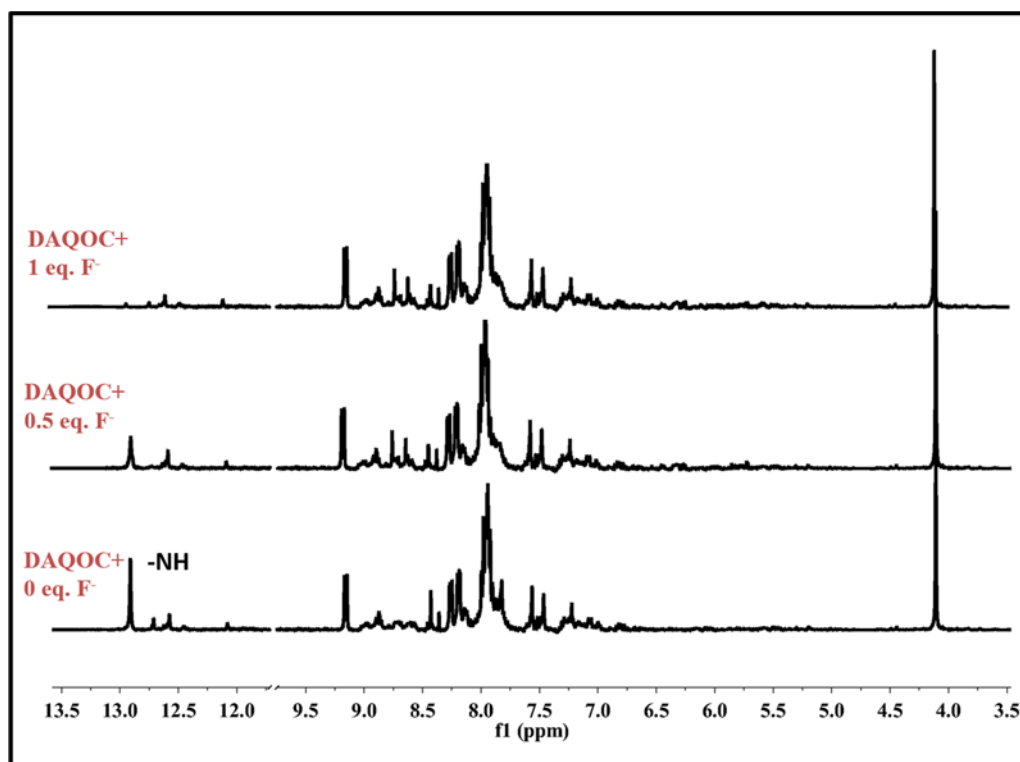


Figure 6. Partial 1H NMR spectra of DAQOC in DMSO solvent upon gradual addition of F^- ions.

3.4 Computational modeling

In an attempt to shed light on structural orientation and identify the mode of fluoride interaction with the DAQOC, Density Functional Theory (DFT) calculations were performed. The unconstrained DFT optimized structure of the DAQOC- F^- complex is given in Figure 7. It can be clearly perceived from the

depiction that the complex was stabilized by the hydrogen bonding interactions contributed by the NH H-bond donors with bond lengths 1.61 and 2.63 Å. However, weaker halogen bonding through the aromatic proton of two opposite rings with bond length of 2.06 and 1.76 Å were also observed. Certainly, it can be rationalized that the acidic protons stabilizes the negative charge of the fluoride ion by classical or non-

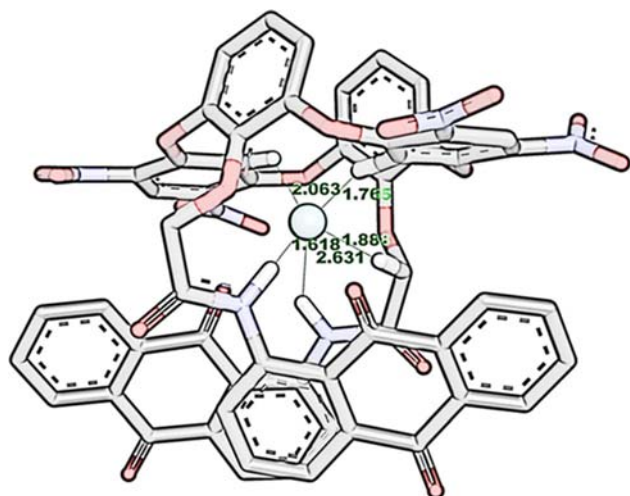


Figure 7. Optimized structure of the complex at B97D/6-31+G* level of theory. Interaction distance from central fluoride anion to donor hydrogens has been enlisted in Å, however remaining hydrogen atoms were omitted for clarity.

classical halogen bondings, in consistent with earlier studies.⁴¹ Around the fluoride ion and the opposite oriented rings of the DAQOC, the non-covalent interactions were also prevalent as depicted in Figure 7. This suggests that the stability of the complex can be exemplified from the mixed interactions of electrostatic and van der Waal types.

Furthermore, the feasibility of the complexation was confirmed by the favourable thermodynamic consideration (Table 1) with enthalpy and free energy change of -129.809 and -121.475 kcal/mol. Subsequently, greater negative complexation values of the interaction energies (-213.758 kcal/mol) were further substantiate the possibility of stable DAQOC-F⁻ complexation. Certainly, this indicates that fluoride generates the complex relying on the potential of stable hydrogen (or halogen) bonds.

NCI Plot calculations as depicted in Figure 8 revealed that the aryl rings (Anion- π) and amide motif of anthraquinone appended oxalix played important

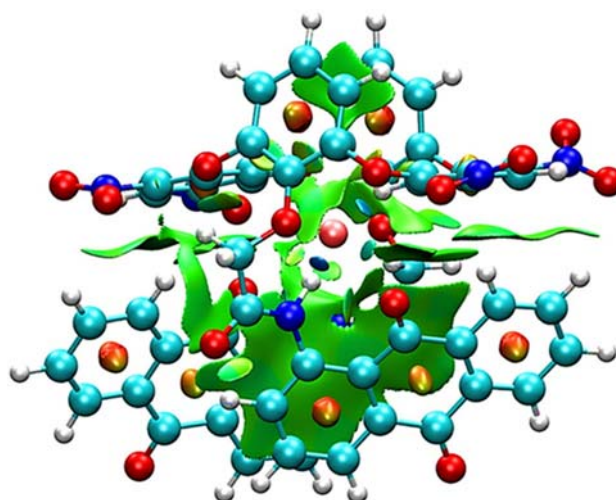


Figure 8. Non-covalent interaction plot for the DAQOC-F⁻.

role in stabilizing the fluoride anions. It is worth mentioning that most of the interactions were contributed from the pi-rings in correspond with earlier study.⁴² The analysis indicated that the appended substituents including nitro groups make the ring electron deficient and thereby more susceptible for the fluoride anion.

3.5 Analytical application

In order to evaluate fluoride ion sensor in an artificial system, the practicality of the DAQOC for real sample analysis was performed. Table 2 shows the estimation of water samples (in the present study, our lab tap water) using standard addition method. The fluoride ion concentration in the water sample was determined from a Stern–Volmer plot as depicted in Figure 5. The recovery of fluoride ions was estimated by spiking the water samples with four different concentrations, i.e., 10 μ M, 20 μ M, 30 μ M, and 40 μ M, of F⁻. Thus, the results demonstrated DAQOC can be used to determine F⁻ in the samples with no significant interferences.

Table 1. Calculated thermochemistry values of the DAQOC-F⁻ complex formation.

Enthalpy Change (ΔH)	Free Energy Change (ΔG)	ΔZPE (kcal/mol/particle)	Complexation Energy (E_{int})*
-129.809	-121.475	-0.62688	-213.758

All values are in Kcal/mol.

*Energies were computed using counterpoise basis set superposition correction (BSSE).

Table 2. Water sample estimation using the standard addition method.

Water Sample	Spiked Fluoride conc. (μM)	Conc. of Fluoride obtained from (N = 3, mean \pm SD), Fig. 5	Found conc. of Fluoride (μM)	% Recovery
1	0	18.13 \pm 0.03	N/A	N/A
2	10	28.26 \pm 0.17	18.26	101.44
3	20	38.60 \pm 0.43	17.89	99.39
4	30	48.20 \pm 0.84	18.2	101.11
5	40	58.70 \pm 0.89	17.88	99.33

4. Conclusions

In summary, we present a selective and sensitive fluorescent probe, DAQOC bearing two aminoanthraquinone units for the detection of fluoride ions. The fluorescent intensity of DAQOC was significantly quenched with the addition of F^- ions which suggest towards the selective behaviour among various anions. From the outcome of this investigation, we can conclude that anion- π interactions, anthraquinone appended oxacalix[4]arene cavity and nitro groups are pivotal for the specific binding with fluoride anion. The DFT calculations decipher towards the hydrogen bonding interactions contributed by the NH H-bond donors and favourable thermodynamic binding ($\Delta G = -121.475$ kcal/mol). The fluorescence probe, DAQOC has lower detection limit as well as high selectivity towards F^- (1.23 μM). This highly sensitive, selective, easy and cost-effective spectrofluorimetric method will provide great interest for routine analysis of F^- .

Supplementary Information (SI)

Figures S1-S9 are available at www.ias.ac.in/chemsci.

Acknowledgement

The authors thank the financial assistance provided by DST-SERB, New Delhi through the project scheme SERB REF. No EMR/2016/001958. Manoj Vora gratefully acknowledges the financial support received from UGC in the form of Rajiv Gandhi National Fellowship, RGNF-JRF (RGNF-2017-18-SC-GUJ-47048). V. K. Jain would like to acknowledge UGC-Mid Career Award for financial assistance (19-213/2018-BSR). Anita Kongor gratefully acknowledges the financial assistance provided by the Council of Scientific & Industrial Research (CSIR), New Delhi for Research Associateship Fellowship (File No. 09/070 (0073) 2020 EMR-I). Manthan K. Panchal gratefully acknowledges Human Resource Development Group - Council of Scientific & Industrial Research (CSIR), New Delhi for Research Associateship Fellowship (File No. 09/70 (0064) 2K19 EMR-I). The authors also acknowledge

the Central Salt & Marine Chemicals Research Institute (Bhavnagar), Oxygen Healthcare-Ahmedabad (O2h), Sophisticated Analytical Instrument Facility (Panjab University) and Gujarat Forensic Sciences University (Gandhinagar), for providing instrumental facilities and UGC Infonet & Information and Library Network (INFLIB-NET) (Ahmedabad) for e-journals.

References

1. Hein R, Beer P D and Davis J J 2020 Electrochemical anion sensing: supramolecular approaches *Chem. Rev.* **120** 1888
2. Pollick H 2018 The role of fluoride in the prevention of tooth decay *Pediatr. Clin.* **65** 923
3. Pereira A G, Chiba F Y, Mattera, M S d L C, Pereira R F, Nunes R d C A, Tsosura T V S, Okamoto R and Sumida D H 2017 Effects of fluoride on insulin signaling and bone metabolism in ovariectomized rats *J. Trace. Elem. Med. Bio.* **39** 140
4. Kanduti D, Sterbenk P and Artnik B 2016 Fluoride: a review of use and effects on health *Mater. Sociomed.* **28** 133
5. Black R M and Read R W 2007 Environmental and biomedical sample analysis in support of allegations of use of chemical warfare agents *Toxin Rev.* **26** 275
6. Kingery A F and Allen H E 1995 The environmental fate of organophosphorus nerve agents: a review *Toxicol. Environ. Chem.* **47** 155
7. Busschaert N, Caltagirone C, Van Rossom W and Gale P A 2015 Applications of supramolecular anion recognition *Chem. Rev.* **115** 8038
8. Kumar R, Sharma A, Singh H, Suating P, Kim H S, Sunwoo K, Shim I, Gibb B C and Kim J S 2019 Revisiting fluorescent calixarenes: from molecular sensors to smart materials *Chem. Rev.* **119** 9657
9. Mehta V, Panchal M, Modi K, Kongor A, Panchal U and Jain V K 2015 The chemistry of nascent oxacalix [n] hetarene (n \geq 4): a review *Curr. Org. Chem.* **19** 1077
10. Panchal M, Kongor A, Athar M, Modi K, Patel C, Dey, S, Vora M, Bhadresha K, Rawal R, Jha P C and Jain V K 2020 Structural motifs of oxacalix [4] arene for molecular recognition of nitroaromatic explosives: experimental and computational investigations of host-guest complexes *J. Mol. Liq.* 112809

11. Wu J R and Yang Y W 2019 New opportunities in synthetic macrocyclic arenes *Chem. Comm.* **55** 1533
12. Ma J X, Fang X, Xue M and Yang Y 2019 Synthesis, structure, and anion binding of functional oxacalix [4] arenes *Org. Biomol. Chem.* **17** 5075
13. Van Rossom W, Caers J, Robeyns K, Van Meervelt L, Maes W and Dehaen W 2012 (Thio) ureido anion receptors based on a 1, 3-alternate oxacalix [2] arene [2] pyrimidine scaffold *J. Org. Chem.* **77** 2791
14. Hou B Y, Wang D X, Yang H B, Zheng Q Y and Wang M X 2007 Synthesis and structure of upper-rim 1, 3-alternate tetraoxacalix [2] arene [2] triazine azacrowns and change of cavity in response to fluoride anion *J. Org. Chem.* **72** 5218
15. An L, Wang J W, Wang C, Zhou S S, Sun J and Yan C G 2018 2, 3-Ethylene-bridged dihomooxacalix [4] arenes: synthesis, X-ray crystal structures and highly selective binding properties with anions *New J. Chem.* **42** 10689
16. Liu W, Wang Q Q, Huang Z T and Wang D X 2014 Design, structure and anion recognition of larger-rim functionalized oxacalix [2] arene [2] triazine hosts *Tetrahedron Lett.* **55** 3172
17. Augusto A S, Miranda A S, Ascenso J R, Miranda M Q, Félix V, Brancatelli G, Hickey N, Geremia S and Marcos P M 2018 Anion recognition by partial cone dihomooxacalix[4] arene-based receptors bearing urea groups: remarkable affinity for benzoate ion *Eur. J. Org. Chem.* **2018** 5657
18. Panchal M K, Athar M, Jha P C, Kongor A, Mehta V and Jain V K 2017 Quinoline appended oxacalixarene as turn-off fluorescent probe for the selective and sensitive determination of Cu²⁺ ions: a combined experimental and DFT study *J. Lumin.* **192** 256
19. Katz J L, Feldman M B and Conry R R 2005 Synthesis of functionalized oxacalix[4] arenes *Org. Lett.* **7** 91
20. Mehta V, Athar M, Jha P C, Panchal M K, Modi K and Jain V K 2016 Efficiently functionalized oxacalix[4] arenes: synthesis, characterization and exploration of their biological profile as novel HDAC inhibitors *Bioorg. Med. Chem. Lett.* **26** 1005
21. Frisch M J, Trucks G W, Schlegel H B, Scuseria G E, Robb M A, Cheeseman J R, Scalmani G, Barone V, Mennucci B, Petersson G A, Nakatsuji H, Caricato, M, Li X, Hratchian H P, Izmaylov A F, Bloino J, Zheng G, Sonnenberg J L, Hada M, Ehara M, Toyota K, Fukuda R, Hasegawa J, Ishida M, Nakajima T, Honda Y, Kitao O, Nakai H, Vreven T, Montgomery J A, Peralta J E, Ogliaro F, Bearpark M, Heyd J J, Brothers E, Kudin K N, Staroverov V N, Kobayashi R, Normand J, Raghavachari K, Rendell A, Burant J C, Iyengar S S, Tomasi J, Cossi M, Rega N, Millam J M, Klene M, Knox J E, Cross J B, Bakken V, Adamo C, Jaramillo J, Gomperts R, Stratmann R E, Yazyev O, Austin A J, Cammi R, Pomelli C, Ochterski J W, Martin R L, Morokuma K, Zakrzewski V G, Voth G A, Salvador P, Dannenberg J J, Dapprich S, Daniels A D, Farkas, Foresman J B, Ortiz J V, Cioslowski J and Fox D J 2009 Gaussian 09, Revision B.01. Wallingford CT
22. Grimme S 2006 Semiempirical GGA-type density functional constructed with a long-range dispersion correction *J. Comput. Chem.* **27** 1787
23. Athar M, Lone M Y and Jha P C 2017 Investigation of structural and conformational equilibrium of Oxacalix [4] arene: a density functional theory approach *J. Mol. Liq.* **237** 473
24. Boys S F and Bernardi F D 1970 The calculation of small molecular interactions by the differences of separate total energies. Some procedures with reduced errors *Mol. Phys.* **19** 553
25. Boys S and Bernardi F 2002 The calculation of small molecular interactions by the differences of separate total energies. Some procedures with reduced errors *Mol. Phys.* **100** 65
26. Contreras-García J, Johnson E R, Keinan S, Chaudret R, Piquemal J P, Beratan D N, Yang W 2011 NCIPLOT: a program for plotting noncovalent interaction regions *Chem. Theory. Comput.* **7** 625
27. Batista R M, Costa S P and Raposo M M M 2013 Naphthyl-imidazo-anthraquinones as novel colorimetric and fluorimetric chemosensors for ion sensing *J. Photochem. Photobiol. A* **259** 33
28. Jones J E, Kariuki B M, Ward B D and Pope S J 2011 Amino-anthraquinone chromophores functionalised with 3-picoly units: structures, luminescence, DFT and their coordination chemistry with cationic Re (I) dimine complexes *Dalton Trans.* **40** 3498
29. Devaraj S, Saravanakumar D and Kandaswamy M 2007 Dual chemosensing properties of new anthraquinone-based receptors toward fluoride ions *Tetrahedron Lett.* **48** 3077
30. Langdon-Jones E E and Pope S J 2014 The coordination chemistry of substituted anthraquinones: developments and applications *Coord. Chem. Rev.* **269** 32
31. Hoten M, Kojima Y and Ito T 1992 Halochromism of acrylic fibres dyed with some disperse dyes *J. Soc. Dyers Colour.* **108** 21
32. Chen X, Leng T, Wang C, Shen Y and Zhu W 2017 A highly selective naked-eye and fluorescent probe for fluoride ion based on 1,8-naphthalimide and benzothiazole *Dyes Pigm.* **141** 299
33. Gunnlaugsson T, Davis A P, O'Brien J E and Glynn M 2005 Synthesis and photophysical evaluation of charge neutral thiourea or urea based fluorescent PET sensors for bis-carboxylates and pyrophosphate *Org. Biomol. Chem.* **3** 48
34. Bobe S R, Bhosale S V, Jones L, Puyad A L, Raynor A M and Bhosale S V 2015 A near-infrared fluoride sensor based on a substituted naphthalenediimide-anthraquinone conjugate *Tetrahedron Lett.* **56** 4762
35. Poulsen J R and Birks J W 1989 Photoreduction fluorescence detection of quinones in high-performance liquid chromatography *Anal. Chem.* **61** 2267
36. Sood D, Kumar N, Singh A, Tomar V, Dass S K and Chandra R 2019 Deciphering the binding mechanism of noscaphine with lysozyme: biophysical and chemoinformatic approaches *ACS Omega* **4** 16233
37. Inoue H, Hida M, Nakashima N and Yoshihara K 1982 Picosecond fluorescence lifetimes of anthraquinone derivatives. Radiationless deactivation via intra- and intermolecular hydrogen bonds *Open J. Phys. Chem.* **86** 3184
38. Jung H S, Kim H J, Vicens J and Kim J S 2009 A new fluorescent chemosensor for F⁻ based on inhibition of

- excited-state intramolecular proton transfer *Tetrahedron Lett.* **50** 983
39. Maity D, Chakraborty A, Gunupuru R and Paul P 2011 Calix[4] arene based molecular sensors with pyrene as fluoregenic unit: effect of solvent in ion selectivity and colorimetric detection of fluoride *Inorg. Chim. Acta* **372** 126
40. Chawla H M, Shrivastava R and Sahu S N 2008 A new class of functionalized calix [4] arenes as neutral receptors for colorimetric detection of fluoride ions *New J. Chem.* **32** 1999
41. Qureshi N, Yufit D S, Steed K M, Howard J A and Steed J W 2014 Hydrogen bonding effects in anion binding calixarenes *CrystEngComm* **16** 8413
42. Wang D X and Wang M X 2013. Anion- π interactions: generality, binding strength, and structure *J. Am. Chem. Soc.* **135** 892